Available online at www.sciencedirect.com
ScienceDirect
Journal of Organometallic Chemistry 692 (2007) 3307–3315
Journal of Organometallic Chemistry
www.elsevier.com/locate/jorganchem

Mechanism of the cyclization of dimethyl diethynyl silane with selenium tetrabromide: Computational and structural studies, and monitoring

Svetlana V. Amosova [a,*], Vladimir A. Shagun [a], Alexander V. Martynov [a], Natalia A. Makhaeva [a], Lyudmila I. Larina [a], Konstantin A. Lysenko [b], Mikhail G. Voronkov [a]

[a] A.E. Favorsky Institute of Chemistry, Siberian Branch of the Russian Academy of Sciences, Irkutsk, 1, Favorsky 664033, Russia
[b] A.N. Nesmeyanov Institute of Organoelement Compounds of RAS, Moscow, 28, Vavilov Str. 119991, Russia

Received 30 October 2006; received in revised form 16 January 2007; accepted 16 January 2007
Available online 23 January 2007

Abstract

The structure of 2,4-dibromo-2-dibromomethyl-3,3-dimethyl-1-selena-3-silacyclopentene-4, formed by regioselective electrophilic addition of $SeBr_4$ to dimethyl diethynyl silane, has been determined using X-ray analysis technique. Quantum chemistry methods were used to study elementary stages of the reaction. It was found that the first stage consisted of $SeBr_4$ conversion into bimolecular complex $Br_2\cdot\cdot SeBr_2$, initiated by dimethyl diethynyl silane. Possible formation of five-membered and six-membered heterocycles involves different cyclization mechanisms. The formation of only five-membered heterocycle is explained by kinetically preferable ring closure through four-center transition state. The conclusions obtained by calculations were confirmed by monitoring of the reaction using ^1H NMR method.

Keywords: Chalcogens; Five-membered unsaturated heterocycles; Reaction mechanisms; NMR spectroscopy; X-ray diffraction

1. Introduction

Saturated sulfur-silicon containing heterocycles [1] including five-membered ones are known from the literature [2a,2b,2c]. Previously we have briefly reported on the synthesis of unsaturated five-membered selenium-silicon containing heterocycle of cyclopentene [3a] structure by the reaction of dimethyl diethynyl silane **1** with selenium tetrabromide. Also this reaction was studied on a series of diethynyl silanes [3b]. But the conclusion about structure of the heterocycle formed was made only on the basis of ^1H, ^{13}C and ^{77}Se NMR methods and GC–MS. At the same time this reaction may involve the cyclization not only into five-membered **2**, but also six-membered heterocycle **4** (Scheme 1). In addition we have found that along with the main reaction product – heterocycle **2**, isolated from the reaction mixture as a crystalline compound, the reaction led to the formation of 3,6-dibromo-4,4-dimethyl-1,4-selenasilafulvene **3** as *Z*- and *E*-isomers (Scheme 1). These heterofulvenes were shown earlier to be the products of the reaction of silane **1** with $SeBr_2$ [4]. The present work deals with the mechanism of new reaction of $SeBr_4$ with silane **1**, which affords the heterocycle **2**. We are going to determine also if the heterofulvene **3** is an intermediate during the formation of heterocycle **2**.

2. Results and discussion

2.1. XRD analysis

The structure of the main product, formed in the reaction of diethynyl silane **1** with $SeBr_4$, was identified by X-ray analysis of the crystalline compound obtained by slow

* Corresponding author. Fax: +3952 42 58 85.
E-mail address: amosova@irioch.irk.ru (S.V. Amosova).

0022-328X/$ - see front matter © 2007 Elsevier B.V. All rights reserved.
doi:10.1016/j.jorganchem.2007.01.023

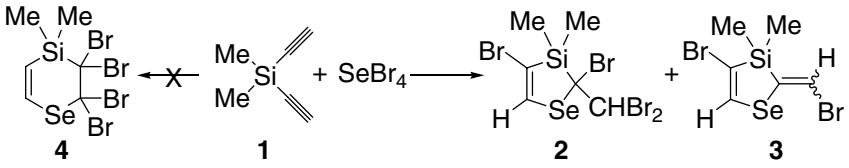

Scheme 1.

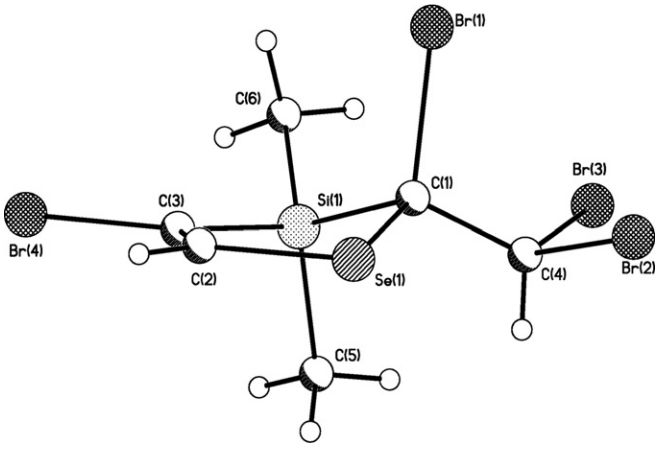

Fig. 1. Molecular structure of heterocycle **2**.

crystallization from chloroform. It was shown that this product is 2,4-dibromo-2-dibromomethyl-3,3-dimethyl-1-selena-3-silacyclopentene-4 (**2**).

The principal geometrical parameters in heterocycle **2** (Fig. 1) are listed in Table 1. Although the direct comparison of bond lengths in **2** is impossible since it is a first structurally characterized compound with 1-selen-3-silacyclopentene-4 fragment we can mention that lengths of endocyclic Se–C bonds in **2** are close to literature data for diselenium analogue [5].

The silicon atom Si(1) is characterized by slightly distorted tetrahedral configuration with the decrease of endocyclic C(1)Si(1)C(3) angle to 95.6(2)° (Table 2). The five-membered ring is characterized by envelope conformation with the deviation of C(1) atom from the plane of Si(1), Se(1), C(2) and C(3) atoms by 0.54 Å. The analysis of crystal packing has revealed that molecules in crystal are assembled into centrosymmetric dimers by means of secondary Br(1)···Br(4)′ ($-x$, $1-y$, $1-z$) (3.544 Å) interactions (Fig. 2). Taking into account the specific directionality of this contact (angle C(1)Br(1)···Br(4′) is equal to 170.3°) as well as elongation of C(1)–Br(1) bond up to 1.971(5) Å we can assume that this contact corresponds to the charge transfer from the electron lone pair (n) of Br(4) atom to antibonding orbital (σ^*) of C(1)–Br(1) bond, i.e. n–σ^* interaction.

Table 1
Bond lengths (Å) in heterocycle **2**

Atom(1)–Atom(2)	Å	Atom(1)–Atom(2)	Å
Si(1)–C(5)	1.834(6)	Br(1)–C(1)	1.971(5)
Si(1)–C(6)	1.841(5)	Br(2)–C(4)	1.946(6)
Si(1)–C(3)	1.870(6)	Br(3)–C(4)	1.924(6)
Si(1)–C(1)	1.917(5)	Br(4)–C(3)	1.903(6)
Se(1)–C(2)	1.909(6)	C(1)–C(4)	1.501(7)
Se(1)–C(1)	1.960(5)	C(2)–C(3)	1.302(7)

2.2. Computational results

To elucidate the reaction mechanism and to explain the formation of only five-membered heterocycle **2** we have carried out quantum chemical computation of possible

Table 2
Valence angles (°) in heterocycle **2**

Angle	ω (°)	Angle	ω (°)
C(5)–Si(1)–C(6)	111.3(3)	C(4)–C(1)–Br(1)	109.5(4)
C(5)–Si(1)–C(3)	109.0(3)	Si(1)–C(1)–Br(1)	107.0(3)
C(6)–Si(1)–C(3)	113.6(2)	Se(1)–C(1)–Br(1)	109.8(2)
C(5)–Si(1)–C(1)	110.0(3)	C(3)–C(2)–Se(1)	118.5(5)
C(6)–Si(1)–C(1)	116.3(3)	C(2)–C(3)–Si(1)	118.5(4)
C(3)–Si(1)–C(1)	95.6(2)	C(2)–C(3)–Br(4)	120.1(4)
C(2)–Se(1)–C(1)	93.8(3)	Si(1)–C(3)–Br(4)	121.4(3)
C(4)–C(1)–Si(1)	115.5(4)	C(1)–C(4)–Br(3)	113.3(4)
C(4)–C(1)–Se(1)	108.6(4)	C(1)–C(4)–Br(2)	114.0(4)
Si(1)–C(1)–Se(1)	106.4(2)	Br(3)–C(4)–Br(2)	110.0(3)

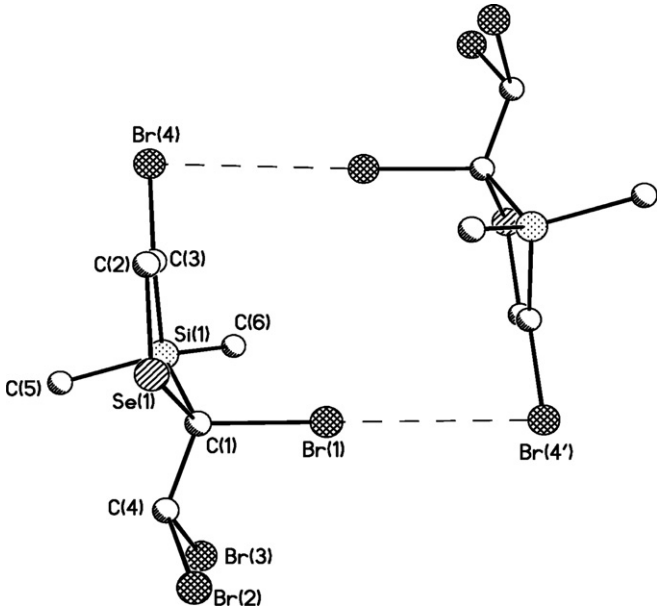

Fig. 2. The centrosymmetric dimers in crystal of **2** (H atoms omitted for clarity).

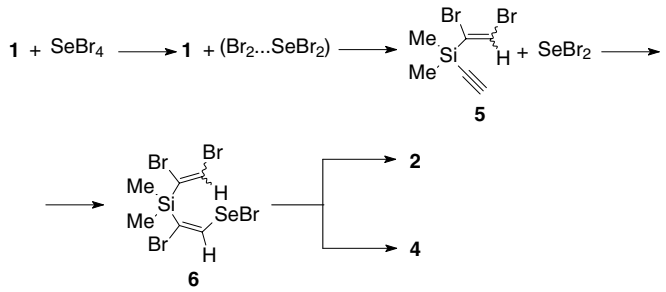

Scheme 2.

routes of the $SeBr_4$ interaction with dimethyl diethynyl silane **1**.

As is seen from the potential energy surface (PES) analysis, the first stage of the reaction involves conversion of $SeBr_4$ into a complex containing molecular bromine and $SeBr_2$ (Scheme 2). The participation of dimethyl diethynyl silane **1** in this process bears evidence of the pronounced catalytic effect. The computations show that in isolated state $SeBr_4$ is thermodynamically less stable than the bimolecular complex $Br_2\cdots SeBr_2$ ($\Delta H = 8.7$ kJ/mol, Fig. 3, Table 3). It is known that in nonaqueous solvents $SeBr_4$ exists as an equilibrium mixture of $SeBr_2$ and Br_2 [6]. The elimination of Br_2 proceeds through the transition state TS1 (Fig. 3, Table 3) with overcoming of 123.1 kJ/mol activation barrier. During the reaction of $SeBr_4$ with diethynyl silane **1** the formation of stable states of the pre-reaction bimolecular complex ($SeBr_4\cdots$**1**) may occur due to different intermolecular interactions of bromine atoms with protons or π-bonds of acetylene moieties of silane **1**. Three lowest states are found on the potential energy surface (Table 3, Fig. 4, structures ($SeBr_4$ + **1**)a–c). The differences in their thermodynamic stability taking into account zero-point vibrations error (ZPVE) are insignificant (Table 3). The values of the interconversion activation energy do not exceed 18 kJ/mol. In every identified state (a–c) the silane molecule **1** initiates the decomposition of $SeBr_4$ into Br_2 and $SeBr_2$, converting the pre-reaction complex ($SeBr_4$ + **1**) into more thermodynamically ($\Delta H = 5$–20 kJ/mol, Table 3) stable state ($Br_2\cdots SeBr_2$ + **1**)a–c (Fig. 4). Activation barriers of these transitions as compared to the gas-phase one (TS1) decrease drastically. Their values do not exceed 40 kJ/mol, which is indicative of considerable impact of the silane **1** on elimination of Br_2 from $SeBr_4$. In Fig. 4, is shown the structure of the transition state (TS2) of the

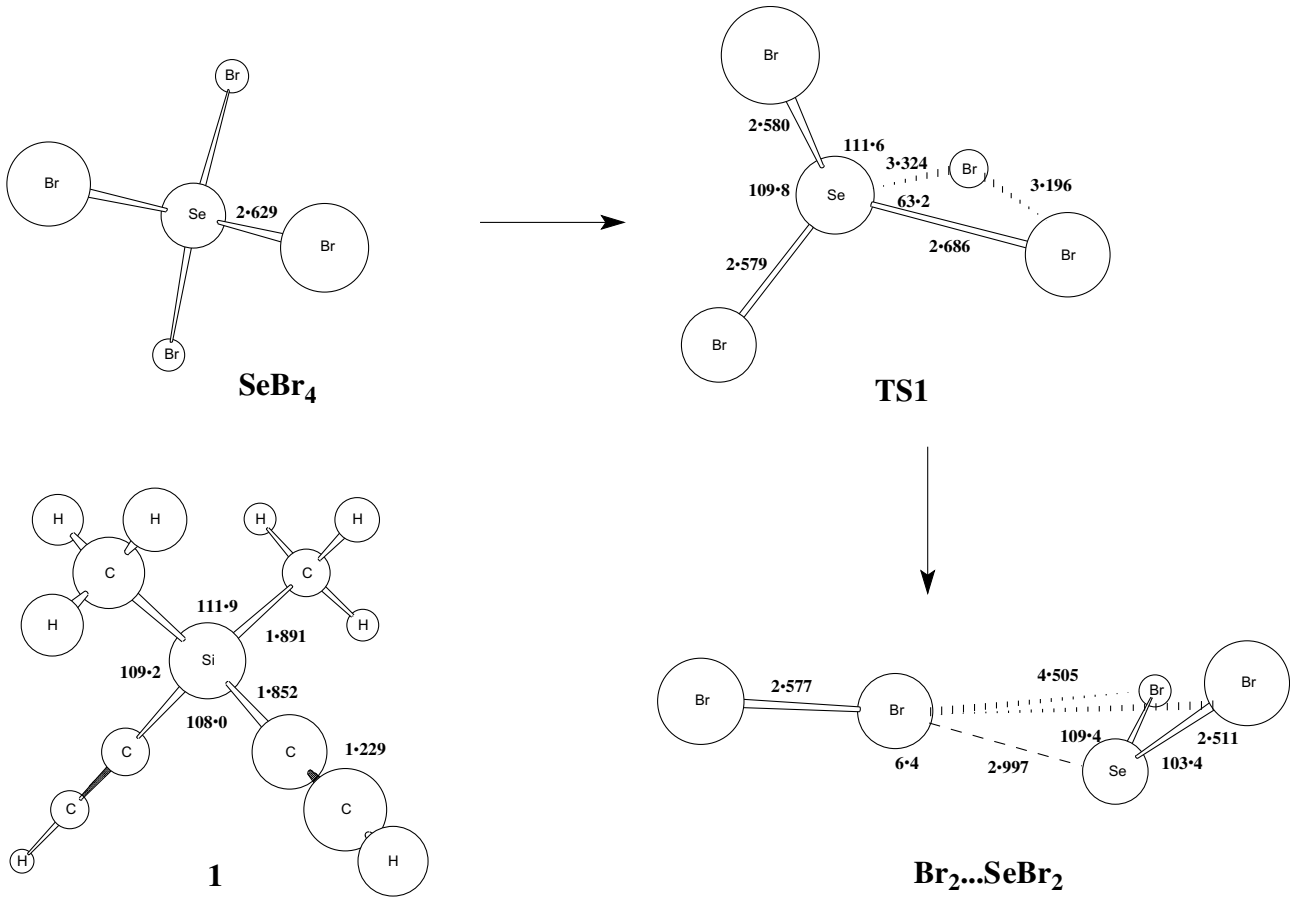

Fig. 3. Molecular structures and basic geometrical parameters of $SeBr_4$, dimethyl diethynyl silane **1**, bimolecular complex $Br_2\cdots SeBr_2$ and transition state (TS1) of the conversion $SeBr_4 \rightarrow Br_2\cdots SeBr_2$, according to B3LYP/LANL2DZ data. Here and Figs. 4, 5, 7 bond lengths are in Å, valence angles in grad.

Table 3
Total energies (E_{tot}, a.e.)[a], zero-point vibration energies (ZPVE, a.e.), relative energies (ΔE, kJ/mol), lowest harmonic frequencies (ω_1, cm^{-1}) and dipole moments (μ, D) of the initial compounds $SeBr_4$ and **1**, complex $Br_2\cdots SeBr_2$, the most stable states (a–c) of bimolecular ($SeBr_4 + \mathbf{1}$) and trimolecular ($Br_2\cdots SeBr_2 + \mathbf{1}$) complexes and transition states TS1 и TS2, according to B3LYP/LANL2DZ data

Structure	$-E_{tot}$	ZPVE	ΔE	ω_1,	μ,
$SeBr_4$	61.85975	0.00234	8.7	39	0.00
$SeBr_2\cdots Br_2$	61.86313	0.00242	0.0	14	0.90
$SeBr_4 \rightarrow SeBr_2\cdots Br_2$ TS1	61.81230	0.00182	131.8	i224	1.72
1	237.21061	0.11420	–	95	0.62
($SeBr_4 + \mathbf{1}$)a	299.07065	0.11675	215.8[b]	6	0.68
($SeBr_4 + \mathbf{1}$)b	299.07048	0.11674	216.3	3	0.78
($SeBr_4 + \mathbf{1}$)c	299.07087	0.11684	215.5	4	0.32
($Br_2\cdots SeBr_2$ +**1**)a	299.07687	0.11711	200.5	12	4.42
($Br_2\cdots SeBr_2 + \mathbf{1}$)b	299.07274	0.11735	211.9	11	3.02
($Br_2\cdots SeBr_2 + \mathbf{1}$)c	299.07878	0.11698	195.1	18	4.19
($SeBr_4$+ **1**)c → ($Br_2\cdots SeBr_2$+ **1**)c TS2	299.05619	0.11651	253.1	i127	2.46

[a] 1a.e. = 2622.9897 kJ/mol.
[b] Reference point – critical point on PES, corresponding to steady state of the structure **4** (Table 4).

rearrangement ($SeBr_4 + \mathbf{1}$)c → TS2 → ($Br_2\cdots SeBr_2 + \mathbf{1}$)c. Activation energy of this process is 37.6 kJ/mol (Table 3). Charge separation degree in the transition states and to a greater extent in the obtained complexes ($Br_2\cdots SeBr_2 + \mathbf{1}$)a–c as compared to the starting states ($SeBr_4 + \mathbf{1}$)a–c (judging by the values of dipole moments, Table 3) increases sharply. This means that on transition from gas phase to condensed media of various polarity the probability of the transition $SeBr_4 + \mathbf{1} \rightarrow Br_2\cdots SeBr_2 + \mathbf{1}$ should increase, both thermodynamically and kinetically. The search for gradient reaction routes related to the direct attack of $SeBr_4$ molecule on π-bond of the silane **1**, by interatomic distance Br–C≡C scanning, has failed. In the distance range Br–C≡C from 3.6 to 3.1 Å occurs barrierless transition of the complex into one of the steady states ($Br_2\cdots SeBr_2 + \mathbf{1}$)a–c. Theoretically the initial elementary stage of the reaction in the trimolecular complex ($Br_2\cdots SeBr_2 + \mathbf{1}$) (Scheme 2) may proceed via three routes: the starting attack of Br_2 or $SeBr_2$ at acetylene fragment of the silane **1** (Scheme 3, *1* and *2*, respectively) or one-stage process connected with synchronic attack of the reagents aforementioned on two acetylene moieties of the silane **1** (Scheme 3, route *3*).

Analysis of gradient routes on the PES of the reactions *1* and *2* unambiguously speaks in favor of the mechanism related to diethynyl silane **1** bromination. The heat of transition ($Br_2\cdots SeBr_2 + \mathbf{1}$)c → **5** + $SeBr_2$ is equal to 107.1 kJ/mol, while activation energy for the transition state (TS3) is 58.0 kJ/mol (Table 4, Figs. 5,6). The reaction route *2*, associated with the initial attack of selenium dibromide on acetylenic fragment of silane **1**, is less advantageous (thermodynamically by 23.6 kJ/mol, and kinetically by 43.9 kJ/mol). Activation energy of one-stage mechanism *3* has even higher value (159.2 kJ/mol). The bimolecular complex **5** + $SeBr_2$ with activation barrier of 126.2 kJ/mol (TS3, Fig. 5, Table 4) transforms to the intermediate **6**. Exothermic addition of $SeBr_2$ results in the increase of the reaction heat balance by 73.2 kJ/mol (Table 4, Fig. 6). In the intermediate **6** the chain of heavy atoms of the molecule Se_1–C_2=C_3–Si_4–C_5=C_6 central skeleton is equiprobably curled into left or right spiral, which torsion angles 1–2–3–4, 2–3–4–5 and 3–4–5–6 are ±5.4°, ±48.3° and и ± 29.1°, respectively. This leads to the formation of the five-membered enantiomeric heterocycle **2** with chiral center C_5.

As a main structural constituent of the reaction coordinate for cyclization of the intermediate **6** into five- or six-membered heterocycle may act either dissociation of the Se–Br bond (followed by 1,6- or 1,5-sigmatropic shift of bromine atom in the ion pair) (Scheme 4a), or interatomic contact Se – π-bond C_5=C_6 (with a formation of four-center transient state) (Scheme 4b).

The computations show that according to both thermodynamic and kinetic parameters the six-membered heterocycle **4** is most likely to be formed through the reaction route *a*. Thermodynamic preference of **4** as compared to **2** (judging from total energy values and taking into account ZPVE) is 11.9 kJ/mol (Table 4). The cyclization activation energy **6** → **4** (TS6) equals to 257.9 kJ/mol (Fig. 6) that is 27.3 kJ/mol lower than the activation barrier of cyclization **6** → **2** proceeding by analogous mechanism. Molecular structure of the transition state (TS6) and the product **4** are given in Fig. 7. The study on gradient route of the cyclization *b* related to the scanning of interatomic distance Se–C_5=C_6 has made it possible to localize only one four-center transition state TS5 that led to the formation of five-membered heterocycle **2** (Fig. 7). Steric restrictions on the molecule skeleton deformation prevented localization of the gradient route of four-center mechanism of the transition **6** → **4** (from localization). The cyclization activation energy **6** → TS5 → **2** is equal to 141.2 kJ/mol (Table 4, Fig. 6) that is almost half as less than that of TS6. Obviously, the differences in the mechanisms of cyclization of **6** into **2** or **4** and, hence high differences between the activation parameters are the

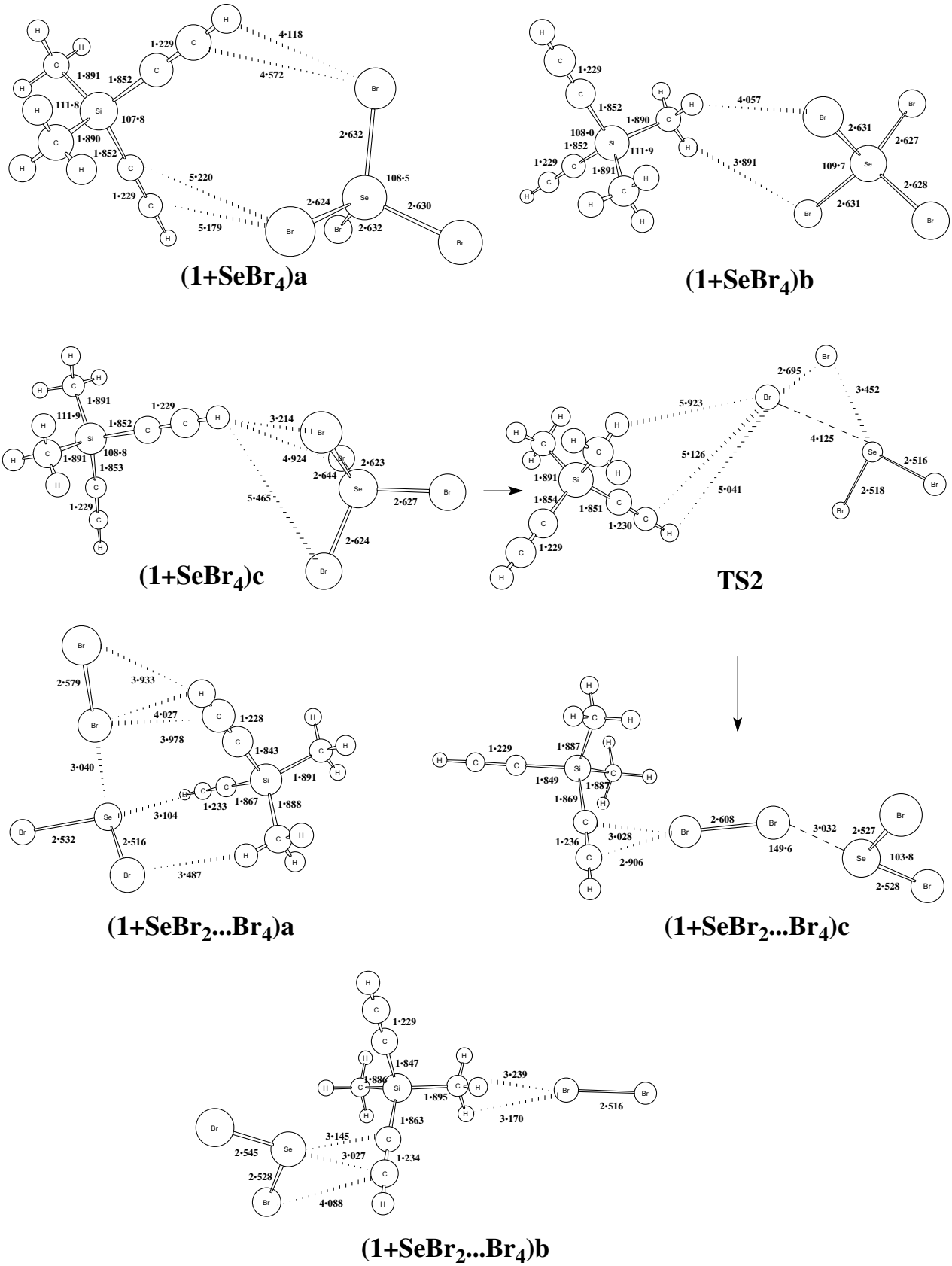

Fig. 4. Molecular structures and basic geometric parameters of the main steady states (a–c) of bimolecular ($SeBr_4 + \mathbf{1}$) and trimolecular ($Br_2\cdots SeBr_2 + \mathbf{1}$) complexes and structure of the transition state (TS2) of the reaction ($SeBr_4 + \mathbf{1}$)c → ($Br_2\cdots SeBr_2 + \mathbf{1}$)c, according to B3LYP/LANL2DZ data.

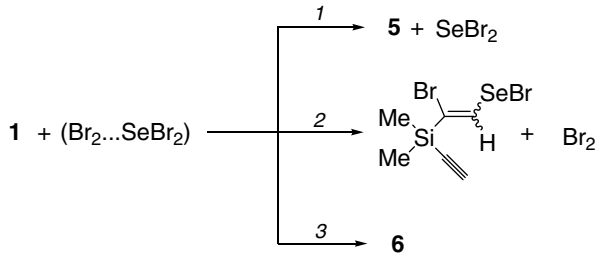

Scheme 3.

prime cause of absolute shift of the products yield towards the heterocycle **2**.

2.3. Monitoring of the reaction by ^1H NMR spectroscopy

Along with the computational methods used for the determination of the reaction mechanism, we also monitored the reaction by ^1H NMR technique at ambient temperature.

Table 4
Total energies (E_{tot}, a.e.), zero-point vibration energies (ZPVE, a.e.), relative energies (ΔE, kJ/mol), virtual and the lowest harmonic frequencies ($i\omega/\omega_1$, cm^{-1}) and dipole moments (μ, D) of heterocycles **2,4** and transition states (TS3–TS6) connecting them, according to B3LYP/LANL2DZ data

Structure	$-E_{tot}$	ZPVE	ΔE	$i\omega/\omega_1$	μ
5	263.57202	0.11831	–	32	2.79
$Br_2\cdots SeBr_2 + 1 \rightarrow$ **5** + $SeBr_2$ TS3	299.07118	0.12286	230.5	i975	4.81
5 + $SeBr_2$	299.12267	0.12004	88.0	3	3.04
5 + $SeBr_2 \rightarrow$ **6** TS4	299.07683	0.12231	214.2	i856	5.23
6	299.15333	0.12278	14.8	11	2.68
6 → **2** TS5	299.09931	0.12258	156.0	i407	5.52
2	299.15548	0.12384	11.9	26	2.15
6 → **4** TS6	299.05870	0.12268	272.7	i317	6.97
4	299.15910	0.12291	0.00	17	2.19

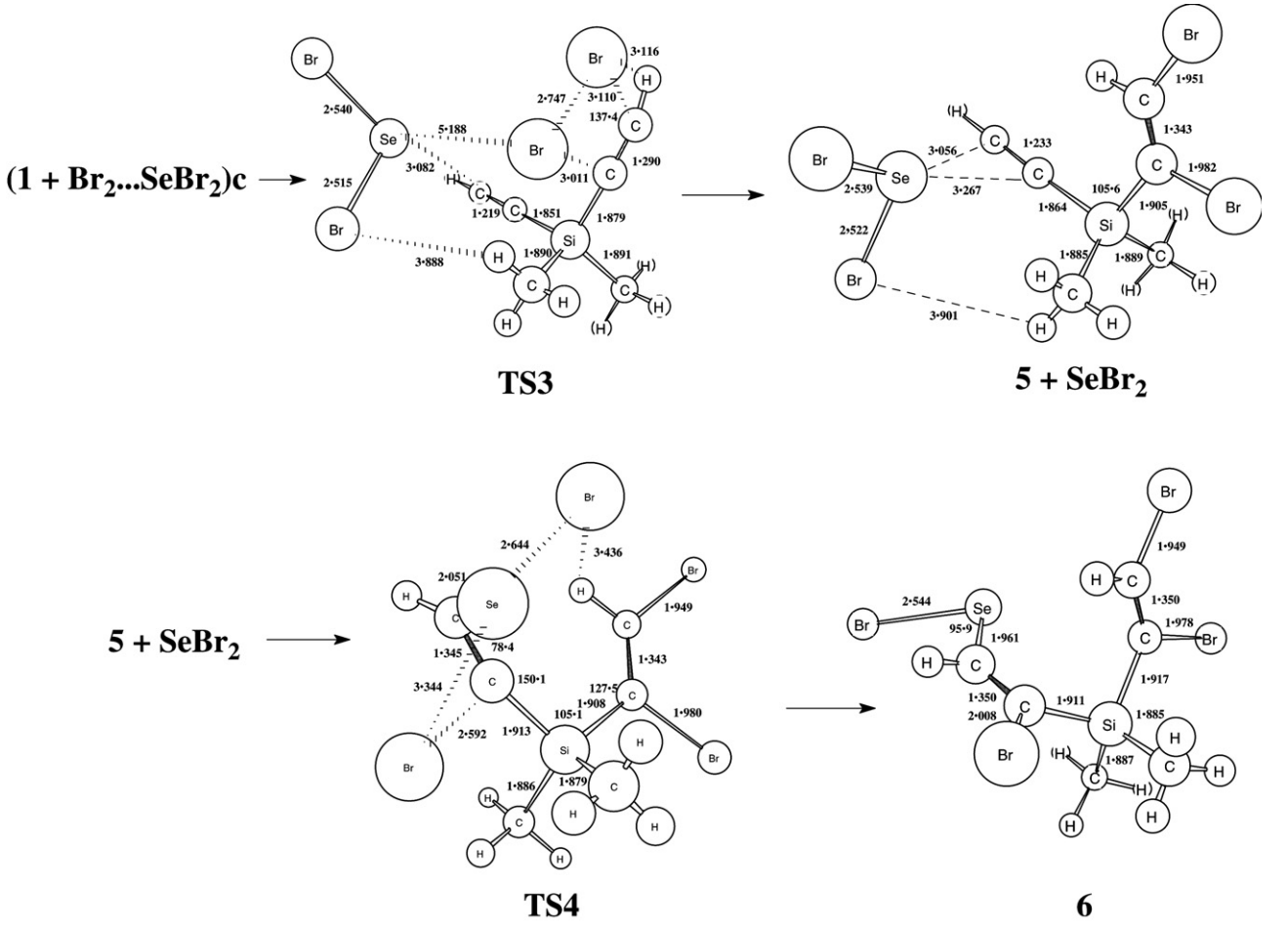

Fig. 5. Basic structural parameters of the transition states (TS3 and TS4) and the reaction products (**5** + $SeBr_2$ and **6**) obtained on modeling (B3LYP/LANL2DZ) of the reaction routes ($Br_2\cdots SeBr_2$ + **1**)c → **5** + $SeBr_2$ and **5** + $SeBr_2$ → **6** correspondingly.

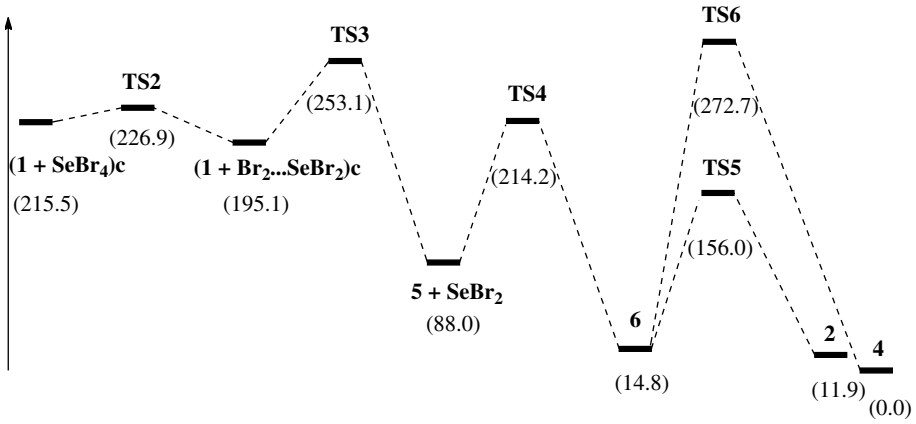

Fig. 6. Schematic energy profile for the reaction of $SeBr_4$ with dimethyl diethynyl silane **1** (the values in parentheses – in kJ/mol).

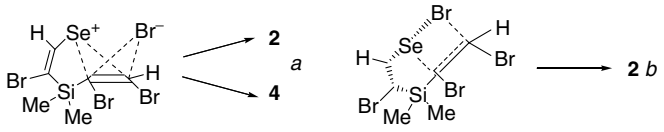

Scheme 4.

The monitoring has been carried out in $CDCl_3$ at room temperature. ^1H NMR spectra were recorded every 5 min during first hour, every 15 min during second hour, every 30 min during the following 1.5 h and every hour during 15 h. Then the monitoring was continued for 48 h with interval of several hours. In the first 15 min NMR spectra of the reaction mixture show wide singlet signals at δ 7.99, 7.90 and 7.40 ppm. (Fig. 8) of low intensities which are probably due to the intermediate compounds **5** and **6** formed immediately after the reagents mixing. The formation of cyclopentene heterocycle **2**, which is characterized by olefin and dibromomethyl proton signals at δ 7.42 and 6.47 ppm [3a], is observed in 15 min after the reaction beginning. While the relative intensity of cyclopentene **2** signals increases, the intensities of signals at δ 7.99, 7.90 and 7.40 ppm drop, which is in good accordance with the decrease of relative concentration of the intermediate compounds during accumulation of the target product. Consequently, due to the presence of $SeBr_2$ in the reaction mixture, a competitive reaction of this reagent with silane **1** occurs that leads to the formation (in 12 h) of 3,6-dibromo-4,4-dimethyl-1,4-selenasilafulvene **3** as *Z*-isomer showing typical doublet signals at δ 7.42 and 6.92 ppm and values of cross-coupling constant $^5J_{HH}$ 1.0 Hz. The formation of *E*-isomer of heterofulvene **3** in negligible amount is detected by the appearance of the corresponding singlet signals at δ 7.34 and 6.82 ppm only on the last stages of the monitoring in 27 h after the reaction beginning. The reaction of $SeBr_2$ with silane **1** and spectral characteristics of heterofulvene **3** isomers formed have been described earlier [4].

The monitoring data (Fig. 8) show that during all time of observation (66 h) the initial diethynyl silane **1** is presented in the reaction mixture. Its content decreases gradually, while it is converted into the reaction main product – heterocycle **2** as well as into the side product – heterofulvene **3**.

Thus, the monitoring data are in good accordance with the computational scheme of the reaction explaining exclusive formation of five-membered heterocylce of cyclopentene structure and testify that cyclopentene heterocycle **2** is formed independently of the heterofulvene **3.**

3. Experimental

^1H (400.1 MHz), ^{29}Si (79.5 MHz) ^{77}Se (70.6 MHz) NMR spectra of the compounds **2** and **3** were recorded in $CDCl_3$ solution with HMDS or $CHCl_3$ (for ^{29}Si NMR spectrum) as internal standards.

*3.1. The reaction of dimethyl diethynyl silane **1** with $SeBr_4$*

Powdered selenium (0.10 g, 1.3 mmol) in $CDCl_3$ (8 ml) was mixed with a bromine solution (0.41 g, 2.5 mmol) in $CDCl_3$ (8 ml) for 2 h, and then a solution of dimethyl diethynyl silane **1** (0.14 g, 1.3 mmol) in $CDCl_3$(5 ml) was added to the reaction mixture. A sample was selected to monitor the reaction using ^1H NMR technique. The reaction mixture was allowed to stand for 66 h at room temperature. The solvent was distilled off in vacuum to give 0.73 g of the mixture containing (^1H NMR data), 2,4-dibromo-2-dibromomethyl-3,3-dimethyl-1-selena-3-silacyclopentene-4 **2** and *Z*-isomer of 3,6-dibromo-4,4-dimethyl-1,4-selenasilafulvene **3** in 55:45 ratio. ^1H, ^{77}Se, ^{29}Si NMR spectra of the heterocycles **2** and **3** are the same that we reported earlier [3a,4].

The mixture thus prepared was dissolved in 0.1 ml $CHCl_3$ and left in the sealed flask for 1 month. During this time a monocrystal was formed in the flask. It was filtered off the mixture, washed with hexane and dried in vacuum.

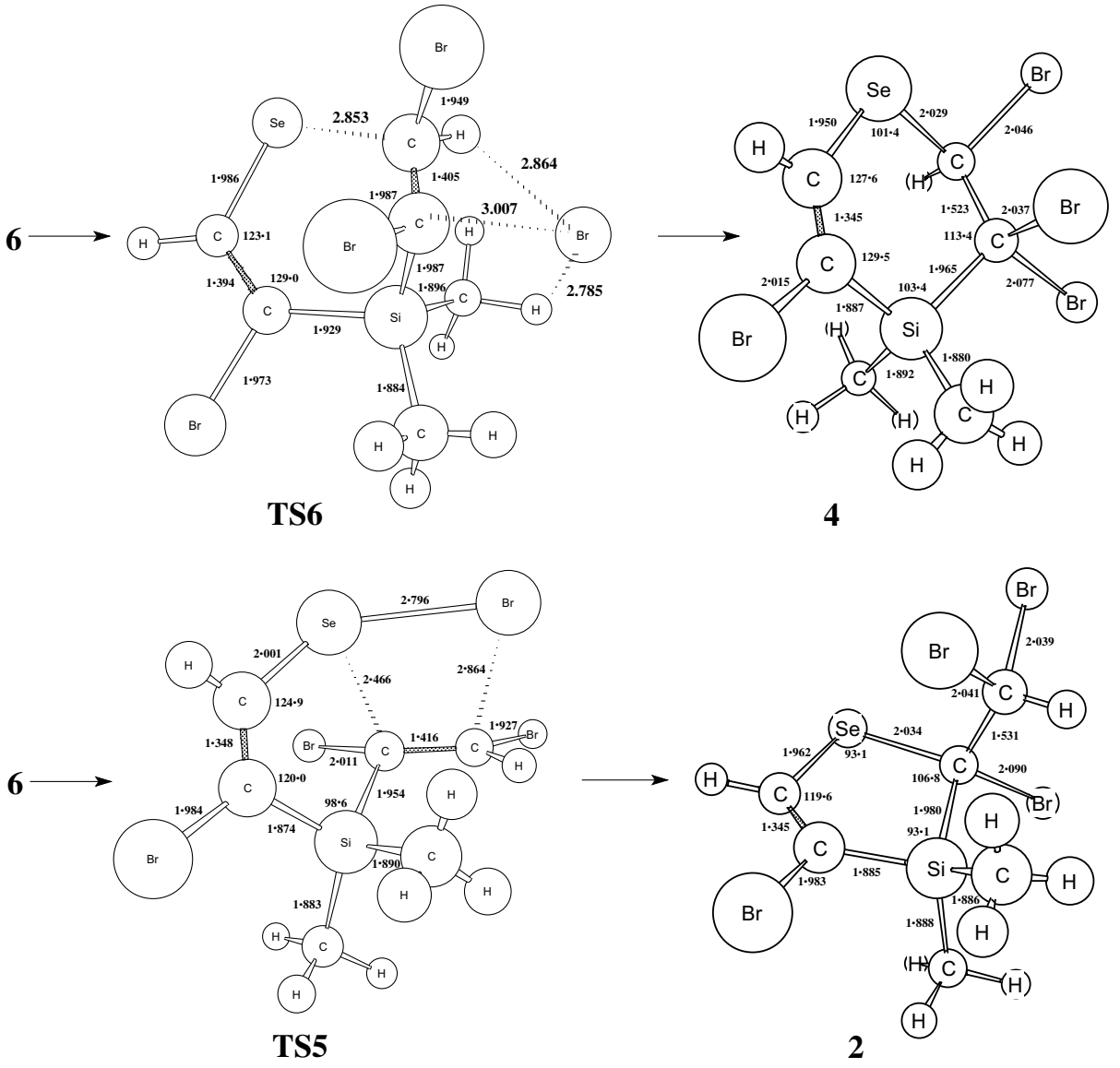

Fig. 7. Basic structural parameters of the transient states (TS5 and TS6) and the reaction products **2** and **4**, according to B3LYP/LANL2DZ data.

*3.2. X-ray analysis of 2,4-dibromo-2-dibromomethyl-3,3-dimethyl-1-selena-3-silacyclopentene- 4 (**2**)*

Crystallographic data for **2**: at 298 K crystals of $C_6H_8Br_4SeSi$ are orthorhombic, space group *Pbca*, $a = 13.408(2)$, $b = 12.2189(19)$, $c = 15.506(3)$ Å, $V = 2540.3(7)$ Å^3, $Z = 8$, $M = 506.81$, $d_{calcd} = 2.650$ g cm^{-3}, μ(Mo Kα) = 155.87, $F(000) = 1856$. Intensities of 30,202 reflections were measured with a Smart CCD diffractometer at 292 K (λ(Mo Kα) = 0.71072 Å, ω-scan technique, $2\theta < 54°$) and 2745 independent reflections ($R_{int} = 0.0816$) were used in further refinement. The structure was solved by direct method and refined on F^2 by a full-matrix least-squares technique in the anisotropic-isotropic approximation. The absorption correction was applied semiempirically from equivalents. Hydrogen atoms were located from the Fourier synthesis and refined in the isotropic approximation in the riding model. The refinement converged to $wR_2 = 0.0887$ and GOF = 0.980 for all independent reflections ($R_1 = 0.0353$ was calculated against F for 1464 observed reflections with $I > 2\sigma(I)$). All calculations were performed using SHELXTL PLUS 5.0.

3.3. Quantum-chemical calculation of the reaction $Me_2Si(C{\equiv}CH)_2$ with $SeBr_4$

DFT/B3LYP method with LANL2DZ basis of the program complex GAUSSIAN-98W has been used for calculation [7]. Geometry full optimization of the molecular systems corresponding to the transition structures ($\lambda = 1$, where λ – number of negative eigenvalues of the Hessian matrix in the given critical point) and energy minima ($\lambda = 0$) on the PES was carried out till the value 10^{-5} Hartree/Bohr. On analyzing flat sites of

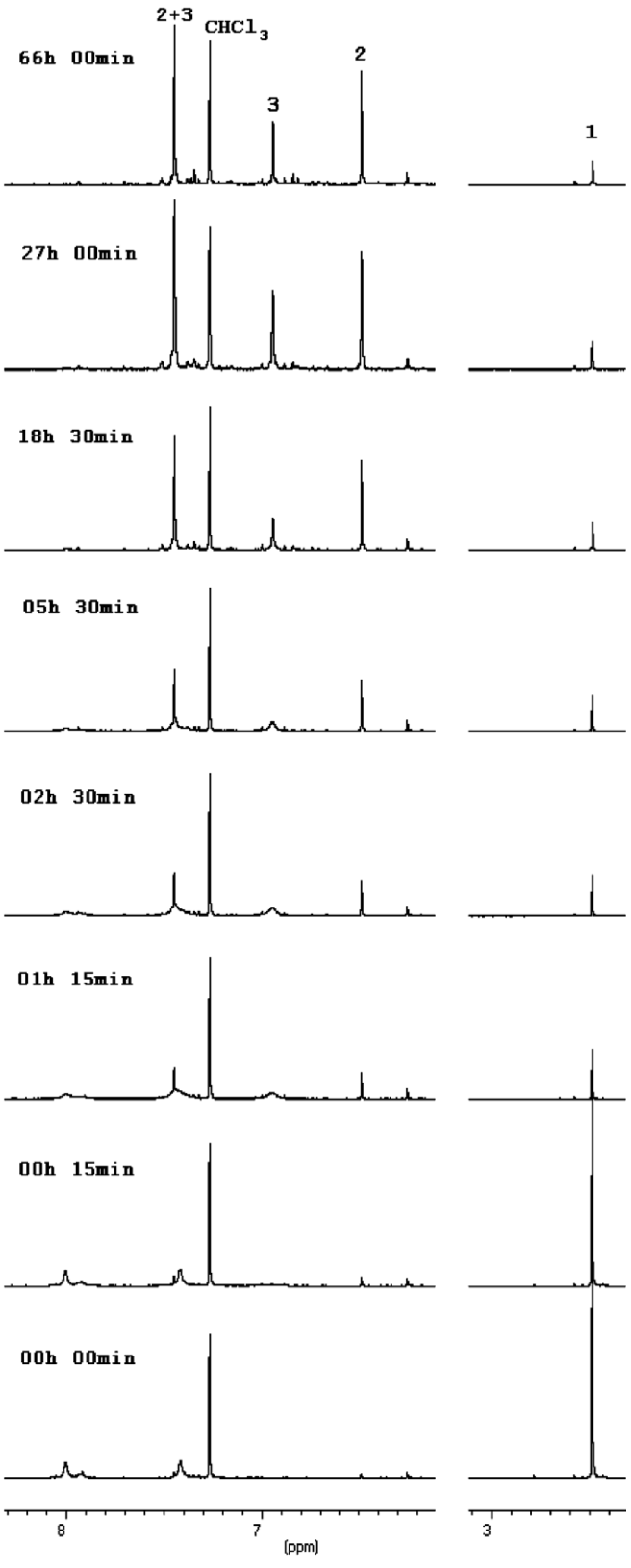

Fig. 8. Time-dependent NMR ^{1}H (400 MHz, $CDCl_3$) at 20 °C for the reaction of **1** with $SeBr_4$. The peak at δ 2.45 ppm is due to ≡CH of **1**, the peaks at δ 6.47 and 7.42 ppm are due to $CHBr_2$ and endocyclic =CH of **2**, the peaks at 6.92 and 7.43 ppm are due to exocyclic and endocyclic =CH of **3.**

the PES during study of the conformational labile states the convergence criterion has been installed at level 10^{-6} Hartree/Bohr. Structures corresponding to the energy minima were identified by means of movement along the gradient lines from the Saddle point to the neighboring critical point starting with a small shift alongside the transitional vector. It has allowed finding correctly the gradient path of the reaction [8].

4. Supplementary material

CCDC 624476 contains the supplementary crystallographic data for **2**. These data can be obtained free of charge via http://www.ccdc.cam.ac.uk/conts/retrieving.html, or from the Cambridge Crystallographic Data Centre, 12 Union Road, Cambridge CB2 1EZ, UK; fax: (+44) 1223-336-033; or e-mail: deposit@ccdc.cam.ac.uk.

Acknowledgement

Financial support of this work in 2006 by the Presidium of Russian Academy of Sciences (Grant No. 8.19) is gratefully acknowledged.

References

[1] E. Block, M. Aslam, Tetrahedron 44 (1988) 281.
[2] (a) M.G. Voronkov, S.V. Kirpichenko, E.N. Suslova, V.V. Keiko, A.I. Albanov, J. Organomet. Chem. 243 (1983) 271;
(b) M.G. Voronkov, S.V. Kirpichenko, E.N. Suslova, V.V. Keiko, J. Organomet. Chem. 204 (1981) 13;
(c) M.G. Voronkov, T.J. Barton, S.V. Kirpichenko, V.V. Keiko, V.A. Pestunovich, Russ. Chem. Bull. Int. Ed. 25 (1976) 702.
[3] (a) V.A. Potapov, S.V. Amosova, O.V. Belozerova, A.I. Albanov, O.G. Yarosh, M.G. Voronkov, Chem. Heterocycl. Comp. 39 (2003) 551;
(b) S.V. Amosova, A.V. Martynov, N.A. Mahaeva, O.V. Belozerova, M.V. Penzik, A.I. Albanov, O.G. Yarosh, M.G. Voronkov, J. Organomet. Chem. 692 (2007) 946.
[4] V.A. Potapov, S.V. Amosova, O.V. Belozerova, A.I. Albanov, O.G. Yarosh, M.G. Voronkov, Chem. Heterocycl. Comp. 39 (2003) 549.
[5] See for e.g.: Yu.E. Ovchinnikov, K.A. Potekhin, V.N. Panov, Yu.T. Struchkov, Dokl. Akad. Nauk SSSR (Russ.) 340 (1995) 62.
[6] J. Milne, Polyhedron 4 (1985) 65.
[7] M.J. Frisch, G.W. Trucks, H.B. Schlegel, G.E. Scuseria, M.A. Robb, J.R. Cheeseman, V.G. Zakrzewski, J.A. Montgomery, R.E. Stratmann, J.C. Burant, S. Dapprich, J.M. Millam, A.D. Daniels, K.N. Kudin, M.C. Strain, O. Farkas, J. Tomasi, V. Barone, M. Cossi Mennucci, B. Mennucci, C. Pomelli, C. Adamo, S. Clifford, J. Ochterski, G.A. Petersson, P.Y. Ayala, Q. Cui, K. Morokuma, D.K. Malick, A.D. Rabuck, K. Raghavachari, J.B. Foresman, J. Cioslowski, J.V. Ortiz, B.B. Stefanov, G. Liu, A. Liashenko, P. Piskorz, I. Komaromi, R. Comperts, R.L. Martin, D.J. Fox, T. Keith, M.A. Al-Laham, C.Y. Peng, A. Nanayakkara, C. Gonzalez, M. Challacombe, P.M.W. Gill, B. Johnson, W. Chen, M.W. Wong, J.L. Andres, C. Gonzalez, M. Head-Gordon, E.S. Replogle, J.A. Pople, GAUSSIAN 98, Revision A. u6, Gaussian, Inc, Pittsburgh, PA, 1998.
[8] R.M. Minyaev, Russ. Chem. Rev. 63 (1994) 883.